NEUROSCIENCE

Macro- and microstructural changes in cosmonauts' brains after long-duration spaceflight

Steven Jillings[1,2]*, Angelique Van Ombergen[1,3], Elena Tomilovskaya[4], Alena Rumshiskaya[5], Liudmila Litvinova[5], Inna Nosikova[4], Ekaterina Pechenkova[6], Ilya Rukavishnikov[4], Inessa B. Kozlovskaya[4†], Olga Manko[4], Sergey Danilichev[7], Stefan Sunaert[8], Paul M. Parizel[9], Valentin Sinitsyn[10], Victor Petrovichev[5], Steven Laureys[11], Peter zu Eulenburg[12], Jan Sijbers[13], Floris L. Wuyts[1‡], Ben Jeurissen[13‡]

Long-duration spaceflight causes widespread physiological changes, although its effect on brain structure remains poorly understood. In this work, we acquired diffusion magnetic resonance imaging to investigate alterations of white matter (WM), gray matter (GM), and cerebrospinal fluid (CSF) compositions in each voxel, before, shortly after, and 7 months after long-duration spaceflight. We found increased WM in the cerebellum after spaceflight, providing the first clear evidence of sensorimotor neuroplasticity. At the region of interest level, this increase persisted 7 months after return to Earth. We also observe a widespread redistribution of CSF, with concomitant changes in the voxel fractions of adjacent GM. We show that these GM changes are the result of morphological changes rather than net tissue loss, which remained unclear from previous studies. Our study provides evidence of spaceflight-induced neuroplasticity to adapt motor strategies in space and evidence of fluid shift–induced mechanical changes in the brain.

INTRODUCTION

Spaceflight does not leave the human body unaffected as space crew enters an environment of microgravity, increased radiation, and social isolation. Consequences of microgravity include body fluid redistribution, reduced use of muscles and bones, and sensory disturbances (*1*). Fortunately, the human body is able to adjust to new environments and conditions to maintain physiological homeostasis and ensure proper behavioral output. The brain, in particular, has a tremendous capacity to adapt, through what is known as neuroplasticity. Neuroplasticity can be defined as the adaptive structural and functional changes occurring in the brain during maturation, learning, environmental challenges, and pathology (*2*). How the brain is able to deal with a microgravity environment, however, is still unknown.

Although the effect of spaceflight on the human body has been researched for almost 60 years, scientists have only recently focused their attention on its effects on the human brain (*3*). Particularly the use of neuroimaging techniques, such as magnetic resonance imaging (MRI), has allowed, for the first time, uncovering structural and functional brain changes after spaceflight. Three types of structural alterations have been observed in the brain of space crew. First, gray matter (GM) volume was found to decrease in the frontal and temporal cortex after spaceflight (*4*, *5*). Second, white matter (WM) volume and fractional anisotropy decreases were found in several of the large WM tracts (*4*, *6*). Third, cerebrospinal fluid (CSF) volume changes included ventricular expansion (*7*–*9*), as well as a redistribution of the subarachnoid CSF, with less CSF at the top of the brain and more CSF at the base (*4*, *6*). Functional brain changes after long-duration spaceflight have so far been reported in one case study (*10*) and one group-level study applying functional MRI (*11*). Common changes noted in these functional imaging studies were modifications of the sensorimotor and vestibular activity or connectivity. Despite the increasing evidence of spaceflight-induced alterations in the brain, data on the long-term effects and the recovery course are scarce. Two studies have implemented measurements acquired 7 months after spaceflight, which show some remaining structural changes of the GM, WM, and CSF (*4*, *7*).

It is widely appreciated that most previously established structural brain changes are driven by body fluid redistribution in microgravity, exerting its effect within the cranium (*4*–*7*). This notion suggests a possible link with the neuro-ophthalmic findings that constitute spaceflight-associated neuro-ocular syndrome (SANS). SANS is characterized by optic disk edema, posterior globe flattening, choroidal folds, and hyperopic shifts in refraction (*12*), which have important implications for the health of space crews and their performance during space missions.

Most of the existing structural findings are based on voxel-based morphometry (VBM) or volumetric analyses of conventional anatomical MRI scans. An important limitation of these techniques is that they use spatial information and priors to obtain discrete tissue segmentations rather than measuring the continuous fractions of multiple tissue types in each voxel directly (*13*). As a result, they are sensitive to macroscopic volumetric changes rather than to underlying microscopic changes in the tissue microstructure (*14*). For

[1]Lab for Equilibrium Investigations and Aerospace, Department of Physics, University of Antwerp, Antwerp, Belgium. [2]Physiology of Cognition Research Center, GIGA Consciousness, GIGA Institute, University of Liège, Liège, Belgium. [3]Department of Translational Neurosciences–ENT, University of Antwerp, Antwerp, Belgium. [4]SSC RF – Institute of Biomedical Problems, Russian Academy of Sciences, Moscow, Russia. [5]Radiology Department, National Medical Research Treatment and Rehabilitation Centre of the Ministry of Health of Russia, Moscow, Russia. [6]Laboratory for Cognitive Research, National Research University Higher School of Economics, Moscow, Russia. [7]Gagarin Cosmonauts Training Center, Star City, Moscow Region, Russia. [8]KU Leuven – University of Leuven, Department of Imaging & Pathology, Translational MRI, Leuven, Belgium. [9]Department of Radiology, Royal Perth Hospital and University of Western Australia Medical School, Perth, WA, Australia. [10]Faculty of Fundamental Medicine, Lomonosov Moscow State University, Moscow, Russia. [11]Coma Science Group, GIGA Consciousness, GIGA Institute, University and University Hospital of Liège, Liège, Belgium. [12]Institute for Neuroradiology, Ludwig-Maximilians-University Munich, Munich, Germany. [13]imec-Vision Lab, Department of Physics, University of Antwerp, Antwerp, Belgium.
*Corresponding author. Email: steven.jillings@uantwerpen.be
†Deceased.
‡These authors contributed equally to this work.

example, regarding the GM volume decreases observed in two previous VBM studies (*4*, *5*), it remains unclear whether these can be considered neurodegenerative.

In this work, we directly extract the fraction of multiple tissues in each voxel from a series of diffusion MRI (dMRI) images, using a technique called multitissue spherical deconvolution (*15*). This technique operates on the idea that each tissue type in the brain has a distinct dMRI signal decay as a function of increasing diffusion weighting strength. Hence, we can obtain the tissues' voxel fractions (VFs) in each voxel directly from the dMRI images, reflecting the relative building blocks within each voxel, without relying on spatial information or priors. In addition, the VF can be modulated by multiplying its value by the local volume change observed during spatial normalization. In other words, the modulated VF (mVF) takes into account volume differences between brain scans to investigate changes in the net amount of each tissue type. Here, VF is a value between 0 and 100%, while mVF can exceed 100%. For example, if two pure WM voxels (VF = 100%) would merge into a single voxel after spatial alignment of the MRI scans, that voxel would be characterized by a mVF of 200%.

Using this approach, we investigate longitudinal changes in VF and mVF of GM, WM, and CSF from dMRI data acquired before (= preflight), 9 days after (= postflight), and 7 months after (= follow-up) long-duration spaceflight. The scaling factor used to modulate the VF values is also evaluated across time points, as it provides a measure of volumetric change, irrespective of a particular tissue type. This approach enables, for the first time, the investigation of changes in multiple tissue types within the same voxels, providing detailed information on spaceflight-induced macro- and microscopic changes in the brain. In addition, dMRI data acquired 7 months after the space mission allow us to evaluate the reversibility of potential early postflight changes.

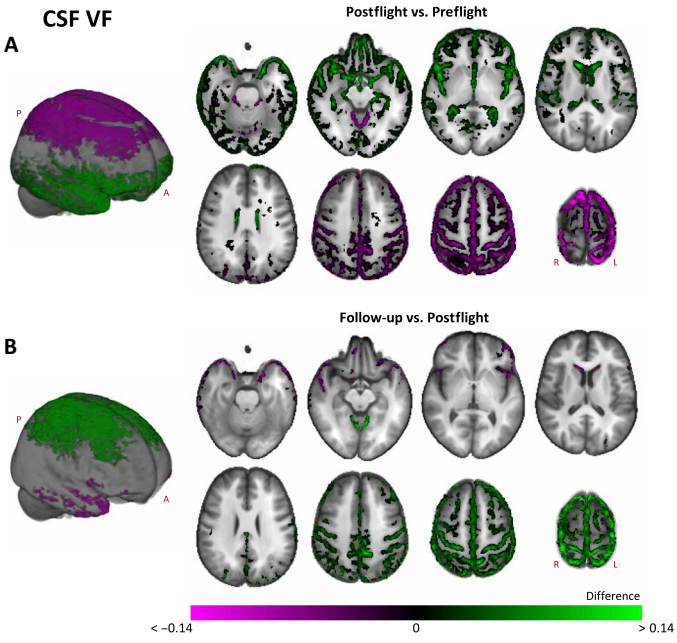

Fig. 1. Whole-brain CSF VF changes from pre- to postflight and from postflight to follow-up. CSF VF increases and decreases from pre- to postflight are shown in (**A**). CSF VF increases and decreases between postflight and follow-up are shown in (**B**). Results from paired *t* tests at a significance threshold of $P < 0.05$ FWE corrected. Background images are averaged images of all subjects in subject-specific template space. Overlaid results are binary on the three-dimensional (3D) volume render and are scaled by the unstandardized effect size (i.e., the difference between two time points) on the axial slices. A, anterior; P, posterior; L, left; R, right.

RESULTS

Whole-brain analysis of brain tissue changes after spaceflight

Spaceflight induces reversible changes in CSF, GM, and WM VFs

Using voxel-based analyses, we evaluated VF changes of CSF, GM, and WM across preflight, postflight, and follow-up, using two-tailed paired *t* tests. All results are statistically thresholded at $P < 0.05$ with family-wise error (FWE) correction.

When comparing post- to preflight, the VF of CSF increased significantly and bilaterally around the inferior parts of the brain, with the largest effects found in the ventricles, along the Sylvian fissures, the anterior temporal lobes, and orbitofrontal lobes (Fig. 1A). Significant decreases were found around superior frontal and parietal areas bilaterally, such as in the longitudinal fissure and (para)central sulci, with the largest effects below the vertex (Fig. 1A). Between postflight and follow-up, a reversal of these effects occurred, i.e., significant decreases of CSF VF in the inferior part and increases in the superior part of the brain (Fig. 1B). This reversal occurred in a larger area at the superior side compared to the inferior side. When comparing follow-up to preflight, no significant differences were found apart from a few isolated voxels in the central sulcus, which showed a remaining decrease in CSF VF.

The GM VF increased significantly between pre- and postflight in the superior frontal and parietal areas bilaterally, with the largest effect occurring below the vertex (Fig. 1A). There was a large overlap between the areas showing GM increases and CSF decreases of VFs. Some areas in the frontal WM also underwent significant VF increases of GM-like tissue (i.e., the GM VF increased in anatomical WM areas). The GM VF decreased significantly and bilaterally along the borders of the Sylvian fissure and of the ventricles, as well as in the temporal poles, which overlapped with a subset of the areas showing increases in CSF VF (Fig. 2A). From postflight to follow-up, GM VF decreased significantly in the superior part of the brain, indicating a reversal of the pre- to postflight effect. However, we also observed more widespread decreases in GM VF in the brain, such as in the posterior temporal lobes (Fig. 2B). We found no significant increases in GM VF from postflight to follow-up nor were any significant differences observed between preflight and follow-up.

The WM VF significantly increased from pre- to postflight in small areas around the pre- and postcentral gyri, as well as in the cerebellar WM. On the other hand, decreases were detected in a few voxels of the temporal and occipital lobes. When comparing follow-up to postflight, WM VF significantly increased in the temporal lobe and decreased in the pre- and postcentral gyri, highlighting the reverse effect (fig. S1). No significant differences were detected between preflight and follow-up.

Spaceflight induces reversible changes in the modulated CSF, GM, and WM VFs

The VF estimates do not take into account potential local differences in volume between subjects and time points. To do so, the VF information in each voxel is scaled by the local volume change to obtain mVFs, which reflect the net amount of each tissue type. Changes in mVF were statistically tested using two-tailed paired *t* tests with a statistical threshold of $P < 0.05$ FWE- corrected.

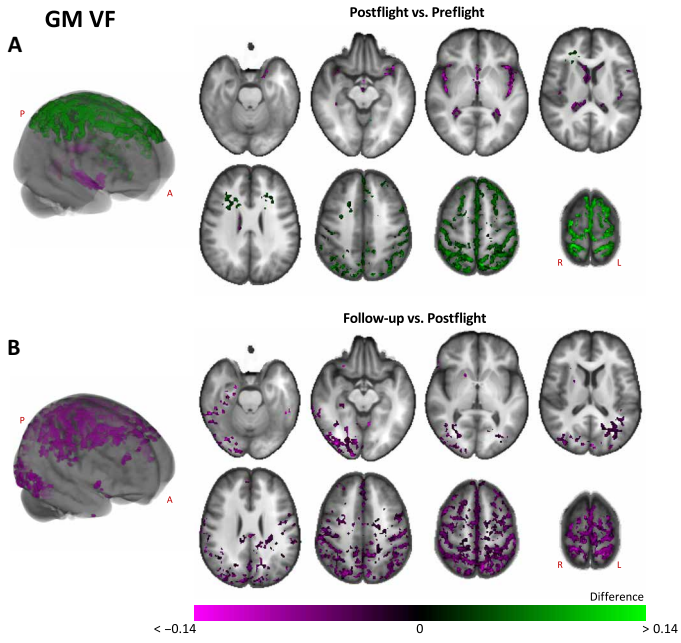

Fig. 2. Whole-brain GM VF changes from pre- to postflight and from postflight to follow-up. GM VF increases and decreases from pre- to postflight are shown in (**A**). GM VF increases and decreases between postflight and follow-up are shown in (**B**). Results from paired *t* tests at a significance threshold of $P < 0.05$ FWE corrected. Background images are averaged images of all subjects in subject-specific template space. Overlaid results are binary on the 3D volume render and are scaled by the unstandardized effect size (i.e., the difference between two time points) on the axial slices. A, anterior; P, posterior; L, left; R, right.

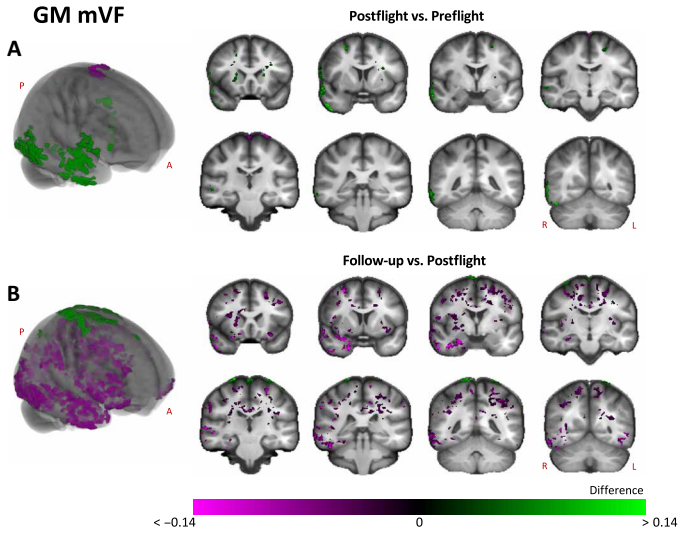

Fig. 3. Whole-brain GM mVF changes from pre- to postflight and from postflight to follow-up. GM mVF increases and decreases from pre- to postflight are shown in (**A**). GM mVF increases and decreases between postflight and follow-up are shown in (**B**). Results from paired *t* tests at a significance threshold of $P < 0.05$ FWE corrected. Background images are averaged images of all subjects in the subject-specific template. Overlaid results are binary on the 3D volume render and are scaled by the unstandardized effect size (i.e., the difference between two time points) on the coronal slices. A, anterior; P, posterior; L, left; R, right.

We found a large overlap between areas showing significant CSF VF and mVF changes (fig. S2). However, while the CSF VF only showed a significant decrease in a small part of the central sulcus when comparing follow-up to preflight, the mVF also remained increased in the lateral and third ventricles for this comparison.

GM mVF increased significantly from pre- to postflight in the right lateral temporal lobe, the basal ganglia, and the superior frontal gyri, with the largest effect detected in the right anterior temporal lobe (Fig. 3A). A small part of the dura mater, including the falx cerebri, showed significantly decreased GM mVF, resulting from the GM-like diffusional properties of this structure (Fig. 3A). When comparing follow-up to postflight, we again observed the reverse effect within the same areas as described for the pre- to postflight comparison. In particular, the mVF of GM-like tissue significantly increased in the dura mater, while it decreased significantly in the right temporal lobe (RTL), as well as in frontal and parietal areas bilaterally, with the largest effect in the anterior temporal lobe (Fig. 3B). No significant differences in GM mVF were observed between preflight and follow-up.

We found significant WM mVF increases in the cerebellum and superior cerebellar peduncle, in the WM around the ventricles, in the internal capsule, and in the precentral gyrus, with the largest effect observed in the cerebellum (Fig. 4A). The WM mVF increases in the cerebellum and precentral gyrus were spatially more extensive than the WM VF increases in these areas. On the other hand, no significant WM mVF decreases were found between pre- and postflight. When comparing follow-up to postflight, WM mVF increased significantly in a few isolated voxels in the brainstem, while it significantly decreased in small areas around the pre- and postcentral gyri, as well as in the cerebellum, highlighting a reversal of the pre- to postflight changes (Fig. 4B). No significant WM mVF differences were detected between preflight and follow-up.

Spaceflight induces local brain volume changes

The scaling factor used to modulate the VF estimates provides a measure for the local volume change of each voxel in the brain, irrespective of a specific tissue type. Therefore, it was used to evaluate voxel expansions and contractions in the brain between preflight, postflight, and follow-up, using two-tailed paired *t* tests, thresholded at $P < 0.05$ FWE-corrected. We found widespread volume increases between pre- and postflight in the ventricles, in the temporal, inferior frontal, and insular cortex, as well as in the cerebellar WM, the internal capsule, and in the WM surrounding the ventricles (fig. S3). The largest increases were found in the anterior insula and ventricles. Significant volume decreases, on the other hand, were found at the superior side of the brain and along the tentorium cerebelli when comparing post- and preflight scans, with the largest effect below the vertex (fig. S3). In these same areas, significant changes in the opposite direction were detected when comparing follow-up to postflight, although only part of the inferior side was reversed. Between preflight and follow-up, the ventricles showed a remaining volume increase. These results overlap largely with the CSF VF and mVF changes, as well as with several areas showing increases in GM and WM mVF.

Brain tissue changes after spaceflight are not attributed to aging

We compared the differences between pre- and postflight MRI in cosmonauts to the differences between two MRI scans obtained with a similar time interval in a control group. We used a two-tailed unpaired nonparametric *t* test to test for statistical differences between cosmonauts and controls (regarding their differences in time).

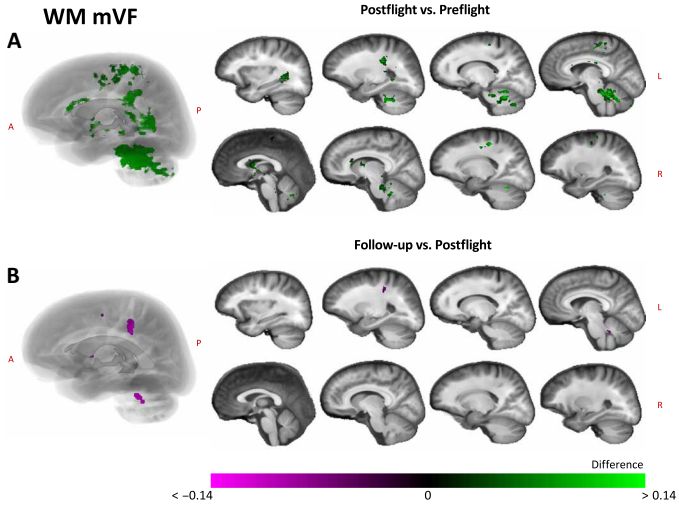

Fig. 4. Whole-brain WM mVF changes from pre- to postflight and from postflight to follow-up. WM mVF increases and decreases from pre- to postflight are shown in (**A**). WM mVF increases and decreases between postflight and follow-up are shown in (**B**). Results from paired *t* tests at a significance threshold of $P < 0.05$ FWE corrected. Background images are averaged images of all subjects in the subject-specific template space. Overlaid results are binary on the 3D volume render and are scaled by the unstandardized effect size (i.e., the difference between two time points) on the sagittal slices. A, anterior; P, posterior; L, left; R, right.

There was no significant difference in age at the time of the first scan between the cosmonaut group and the control group [two-tailed exact Mann-Whitney *U* test, $U = 56.0$, n (cosmonaut) = 13, n (control) = 13, $P = 0.153$] nor in the time interval between the pre- and postflight scan of the cosmonaut group and the two scan sessions of the control group [two-tailed exact Mann-Whitney *U* test, $U = 63.5$, n (cosmonaut) = 13, n (control) = 13, $P = 0.292$].

The results of the voxel-based unpaired *t* tests were highly comparable to those of the paired *t* test in cosmonauts, which provides evidence that the current observations are caused by spaceflight rather than aging (figs. S4 and S5). In general, fewer significant voxels were found for the unpaired *t* tests compared to the paired *t* tests. As opposed to the paired *t* tests, the unpaired *t* tests did not reveal a significant GM mVF decrease in the dura mater nor a significant increase in the basal ganglia. In addition, no significant WM VF differences were found, and the WM mVF was significantly increased in the cerebellum only.

Region of interest–based analyses

We subsequently summarized tissue properties within regions of interest (ROIs) to highlight several relevant quantitative changes that occur as a result of spaceflight. In the next sections, the median of the differences between time points is reported in absolute terms for total GM, WM, and CSF, as well as for the tissue parameters of each ROI, which are expressed as percentages (e.g., 50% − 40% = 10%). On the other hand, ventricular changes and the volume changes of the ROIs are reported as relative changes. All median values are accompanied by the median absolute deviation (MAD) as a measure of spread. The summarized values within each ROI for each time point in the cosmonaut group and for each tissue type tested are found in table S1.

Whole-brain absolute changes of GM, WM, and CSF mVF

First, we evaluated the average GM, WM, and CSF mVF of the whole brain and their changes across time points (fig. S6). The GM mVF in cosmonauts increased by 0.6% (MAD = 0.6%) from preflight to postflight and by 0.2% (MAD = 0.3%) from preflight to follow-up. The WM mVF of the whole brain in cosmonauts increased by 0.1% (MAD = 0.9%) between pre- and postflight and increased by 0.5% (MAD = 0.6%) between preflight and follow-up. Last, the CSF mVF increased by 0.1% (MAD = 0.3%) between pre- and postflight and by 0.3% (MAD = 0.3%) between preflight and follow-up. Linear mixed models were applied on the cosmonaut group including all three time points, which showed a significant effect of time on the total GM ($P = 0.022$). Post hoc tests revealed a significant difference between postflight and follow-up for the whole-brain GM mVF ($P = 0.036$). No significant effect of time was observed on the whole-brain WM ($P = 0.433$) or the CSF ($P = 0.132$) mVF. We also observed a significant interaction effect of group and time for CSF mVF, where the pre- to postflight change in cosmonauts significantly differed from the change between the two control measurements [two-tailed exact Mann-Whitney *U* test, $U = 44$, n (cosmonauts) = 13, n (controls) = 13, $P = 0.039$]. No significant interaction effect was observed for GM or WM mVF.

Relative changes of ventricular CSF mVF

Next, average CSF mVF was calculated in lateral, third, and fourth ventricular compartments and evaluated for relative changes across time. These results reveal a 12.5% (MAD = 7.9%) increase in the lateral ventricle postflight relative to preflight, which remained increased at follow-up relative to preflight by 6.2% (MAD = 2.7%). The third ventricle showed a 10.6% (MAD = 3.0%) increase postflight relative to preflight and a remaining 5.0% (MAD = 1.7%) at follow-up relative to preflight. The fourth ventricle decreased postflight relative to preflight by 1.4% (MAD = 4.3%), while it was increased by 1.6% (MAD = 3.5%) at follow-up relative to preflight. Linear mixed models were applied on the cosmonaut group including all three time points, which revealed a significant effect of time on the CSF change in lateral ($P < 0.001$) and third ($P < 0.001$) ventricular compartments, but not in the fourth ventricle ($P = 0.155$). Post hoc testing revealed a significant increase between pre- and postflight (lateral and third ventricle: $P < 0.001$), between preflight and follow-up (lateral ventricle: $P = 0.015$; third ventricle: $P = 0.003$), as well as between postflight and follow-up for the third ventricle only ($P = 0.004$). We also found a significant interaction effect of group and time, where the pre- to postflight difference in cosmonauts was significantly different from that of the controls for lateral and third ventricles [two-tailed exact Mann-Whitney *U* test, n (cosmonauts) = 13, n (controls) = 13; lateral ventricle: $U = 11$, $P < 0.001$; third ventricle: $U = 3$, $P < 0.001$].

Post hoc ROI analysis

A second aim of this approach was to compare changes in different tissue decompositions within six ROIs based on the voxel-based analysis results between pre- and postflight. First, two ROIs were defined as the overlapping voxels showing opposite significant effects of spaceflight on GM and CSF VF (compare Figs. 1 and 2), one in the superior frontal and parietal regions ("superior CSF interface") and one in the temporal, insular, and ventricular regions ("inferior CSF interface"). Another ROI was defined as the voxels showing significant GM mVF increases in the RTL (Fig. 3A). Three other ROIs were chosen for their potential implications in motor function. Two of these ROIs were defined as the voxels showing significant WM mVF increases at the voxel level, one in the cerebellum, and another in the pre- and postcentral gyri (Fig. 4A). Last, a ROI was defined in the basal ganglia, consisting of the voxels showing GM

mVF increases (Fig. 3A). For the latter four ROIs, in particular, the CSF VF and mVF were scrutinized to assess whether fluid shift effects contributed to the observed findings. The results of the first three ROIs are illustrated in Fig. 5, while the results of the motor ROIs are illustrated in Fig. 6.

In the superior CSF interface, the CSF VF decreased by 6.9% (MAD = 2.1%) and the CSF mVF by 7.3% (MAD = 2.0%), while the GM VF increased by 5.0% (MAD = 1.1%) and the GM mVF by 1.2% (MAD = 0.4%) between pre- and postflight. The volume in this region decreased by 5.2% (MAD = 1.1%) postflight relative to preflight. When follow-up was compared to preflight, the CSF VF was decreased by 0.6% (MAD = 1.0%) and the CSF mVF by 0.3% (MAD = 1.6%), while the GM VF was increased by 0.4% (MAD = 0.8%) and the GM mVF by 1.1% (MAD = 1.0%). The volume was decreased by 1.0% (MAD = 1.7%) for this comparison. These results highlight the opposing changes in GM and CSF VF, driven by a net decrease of the CSF in this region. Our data at follow-up point toward a normalization to baseline.

In the inferior CSF interface, CSF VF increased by 7.6% (MAD = 1.1%) and CSF mVF by 9.4% (MAD = 2.2%), while GM VF decreased by 7.5% (MAD = 1.5%) and GM mVF by 4.6% (MAD = 1.1%) between pre- and postflight. We further found a volume increase of 5.7% (MAD = 2.1%). When comparing follow-up to preflight, CSF VF was increased by 3.6% (MAD = 0.7%) and CSF mVF by 4.8% (MAD = 0.8%), while GM VF was decreased by 2.8% (MAD = 1.6%) and GM mVF was decreased by 1.3% (MAD = 1.0%). The volume of this region was increased by 2.5% (MAD = 0.9%) at follow-up relative to preflight. These findings point to a CSF-driven volume expansion with concomitant decreases of the GM fraction. Our follow-up data indicate a partial normalization of these postflight changes, with some degree of remaining CSF-based volume expansion.

WM mVF of the cerebellum increased by 6.5% (MAD = 0.8%), WM VF by 3.4% (MAD = 0.7%), and volume by 3.7% (MAD = 0.7%) from pre- to postflight. WM mVF remained increased by 3.5% (MAD = 0.9%), WM VF by 1.9% (MAD = 1.3%), and the volume by 1.8% (MAD = 1.4%) when comparing follow-up to preflight. The CSF VF and mVF changes in this ROI were negligibly low. These results indicate a postflight increase in the net amount of WM tissue in the cerebellum, in the WM fraction occupying the voxels in this region, as well as an overall volume increase, while no evidence of fluid alterations was shown in this region.

In the pre- and postcentral gyri, we found that the WM mVF increased by 6.3% (MAD = 2.0%) and the WM VF increased by 4.4% (MAD = 1.5%) from pre- to postflight. Both WM mVF and WM VF remained increased when comparing follow-up to preflight by 2.5% (MAD = 0.7%) and 3.1% (MAD = 0.6%), respectively. There was a volume increase of 1.5% (MAD = 1.4%) in this region postflight relative to preflight and of 0.6% (MAD = 0.4%) follow-up relative to preflight. CSF VF and mVF changes in this ROI were negligibly low. Similar to the cerebellum, the pre- and postcentral gyri exhibited a postflight increase in the WM amount and in the WM fraction occupying this region's voxels, while no contribution of fluid changes in this region was evident.

In the basal ganglia, GM mVF was increased by 5.1% (MAD = 1.6%) and GM VF by 3.1% (MAD = 1.5%) from pre- to postflight. Between preflight and follow-up, GM mVF increased by 1.0% (MAD = 0.5%)

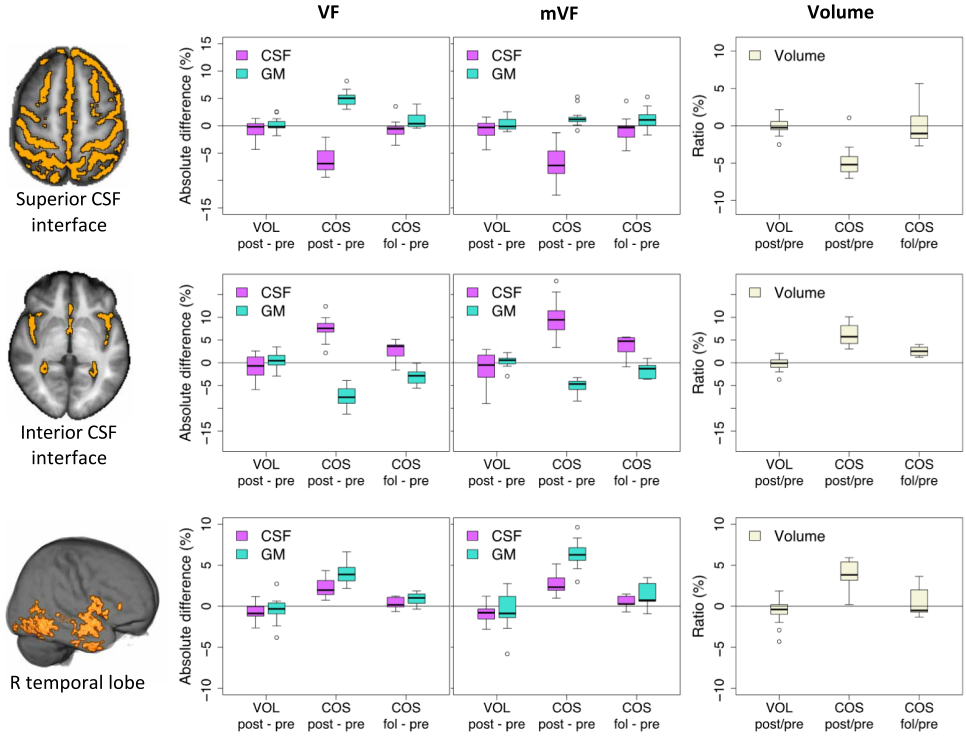

Fig. 5. Relation between GM and CSF changes through ROI-based analysis. ROIs are depicted as binarized images overlaid onto 3D volume renders (**left**). Next to each ROI image, box plots show the differences in tissue VF and tissue mVF between and the volume ratio of (i) the two measurements of the control group volunteers (VOL), (ii) postflight (post) and preflight (pre) in cosmonauts (COS), and (iii) follow-up (fol) and preflight in cosmonauts. The centerline of the box plot indicates the median, the bottom and top edges of the box mark the 25th and 75th percentiles, respectively, and the whiskers extend to the most extreme data points, excluding outliers.

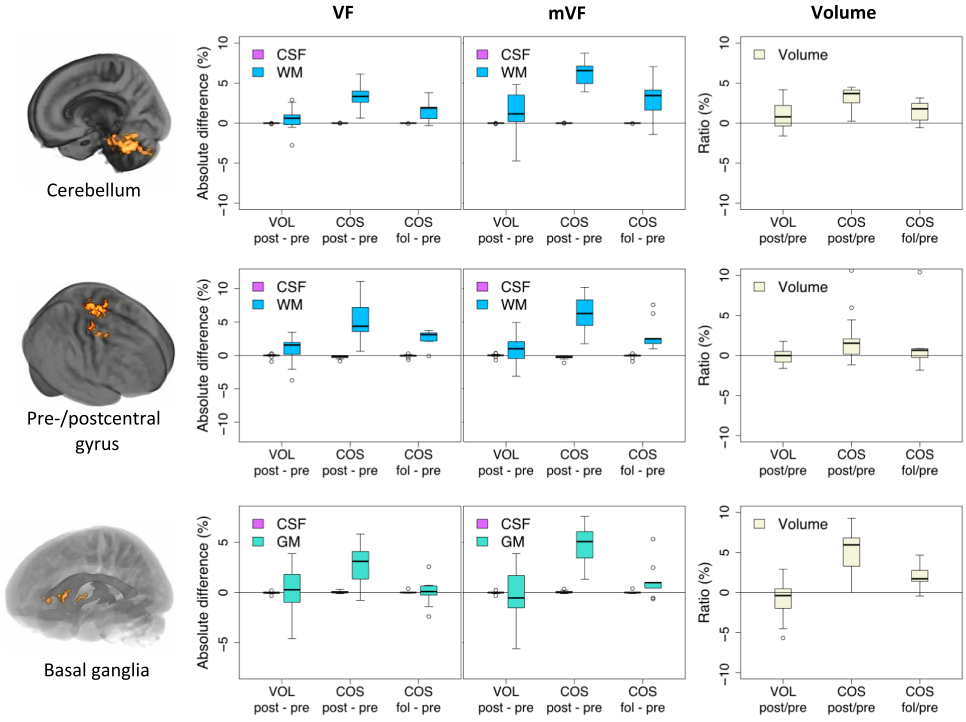

Fig. 6. GM and WM changes in brain motor areas through ROI-based analysis. ROIs are depicted as binarized images overlaid onto 3D volume renders (**left**). Next to each ROI image, box plots show the differences in tissue VF and tissue mVF between and the volume ratio of (i) the two measurements of the control group volunteers (VOL), (ii) postflight (post) and preflight (pre) in cosmonauts (COS), and (iii) follow-up (fol) and preflight in cosmonauts. The centerline of the box plot indicates the median, the bottom and top edges of the box mark the 25th and 75th percentiles, respectively, and the whiskers extend to the most extreme data points, excluding outliers.

and GM VF by 0.1% (MAD = 0.6%). The volume increased by 5.9% (MAD = 1.7%) postflight relative to preflight and remained increased by 1.7% (MAD = 1.1%) at follow-up relative to preflight. CSF mVF and VF changes in this area were negligibly low. These findings point toward a net increase in GM tissue, an increase in the occupying fraction of GM within the basal ganglia's voxels and an overall volume increase, while no effect of fluid changes was evident.

The GM mVF of the RTL increased by 6.3% (MAD = 0.9%) and the CSF mVF by 2.3% (MAD = 0.9%) from pre- to postflight. In addition, the GM and CSF VF were increased from pre- to postflight by 3.9% (MAD = 0.9%) and 2.0% (MAD = 0.7%), respectively, and the RTL volume increased by 3.8% (MAD = 1.4%) postflight relative to preflight. Comparing follow-up to preflight revealed an increase of GM mVF by 0.7% (1.0%), of CSF mVF by 0.3% (MAD = 0.4%), of GM VF by 1.0% (MAD = 0.7%), and of CSF VF by 0.2% (MAD = 0.3%). The RTL volume was decreased by 0.5% (MAD = 0.8%) between preflight and follow-up. These results highlight a postflight volume expansion in the RTL with associated increases in the amount of CSF, which partially sustain up until the follow-up time point. Changes between the two time points of the control group for each ROI had median values that approached 0%. This finding indicates there was no confounding effect of aging.

Visual acuity changes in cosmonauts and correlations with brain tissue changes

We analyzed visual acuity scores between pre- and postflight in cosmonauts and performed a voxel-based correlation analysis between pre- to postflight visual acuity changes and CSF mVF changes. We also performed an ROI-based correlation analysis between visual acuity changes and the CSF mVF changes in the superior and inferior CSF interface ROIs, as well as the lateral and third ventricular compartments. Visual acuity significantly decreased postflight compared to preflight for both the right eye [$P = 0.016$; median change (MAD) = −0.1 (0.1)] and the left eye [$P = 0.014$; median change (MAD) = −0.5 (0.2)].

At the voxel level, we found a significant negative correlation between the relative change in CSF mVF in the lateral ventricle and the pre- to postflight change in visual acuity of the left eye. At the ROI level, visual acuity changes from pre- to postflight in the left eye also correlated significantly and negatively with the relative change of the whole lateral ventricular CSF mVF pre- to postflight (Kendall's tau $b = -0.474$; $P = 0.032$). These results mean that higher ventricular volume increases were associated with larger reductions in visual acuity postflight (fig. S6). No significant changes were observed between visual acuity changes and changes in any other ROI tested.

DISCUSSION

CSF redistribution and GM morphological alterations

In this study, we investigated changes of tissue VFs, mVFs, and volume changes in the brain after long-duration spaceflight both at the voxel level, as well as summarized across voxels in post hoc–defined ROIs. In addition, the reversibility of such effects was assessed by a follow-up measurement, 7 months after return from space. When investigating the CSF tissue changes across time points, we found a nearly complete overlap between voxels showing a change in VF and voxels showing a change in mVF, which were almost exclusively located at interfaces between tissue and CSF. Hence, our findings

point toward net changes in the CSF volume, which lead to alterations in the VFs at these interfaces. When comparing postflight to preflight measurements, the CSF volume increased around the inferior part of the brain, such as in the Sylvian fissure, while it decreased along the superior brain convexity. These findings correspond largely with those of previous studies using VBM (*4*) and free-water analysis of dMRI (*6*). These results point toward a microgravity-induced upward brain shift inside the skull, which is in line with the qualitative observations of Roberts and colleagues (*8*). Our results also point to a cerebellar upward shift, as CSF volume along the tentorium cerebelli was reduced after spaceflight, in line with a narrowing of the supravermian cistern reported in some astronauts in a previous study (*8*). It appears that not only the brain as a whole but also the cerebellum independently is displaced upward in response to microgravity. Furthermore, our results show increased CSF volume at the border of the lateral and third ventricles, which correspond to the established ventricular enlargement after spaceflight (*4*, *7*–*9*).

Previous VBM analyses of GM volume changes after spaceflight have revealed decreases along the inferior frontal and temporal lobes bilaterally (*4*, *5*). Both authors ascribed these findings to fluid shift effects, which was particularly supported by Van Ombergen and colleagues (*4*), as they demonstrated CSF volume increases in combination with the GM volume decreases along the same brain regions. However, it remained unclear whether these GM volumetric changes are merely the result of fluid redistribution or reflect net tissue changes. In the current study, we also show the opposing changes in GM and CSF, but we were additionally able to disentangle changes in VF and mVF of each tissue type within the same voxels. Hence, we found that mainly the VF of GM, and not the mVF, changed along with CSF changes. In particular, the superior part of the brain shows VF increases of GM, which can be explained by the CSF volume decrease in this region, causing crowding of the GM tissue along the interface with the sulci. This gyral crowding has been noted in previous studies as well (*8*, *16*). Similarly, increased CSF volume in the Sylvian fissure and ventricles causes the adjacent GM tissue to be pushed aside, which leads to decreased GM VF estimates, without pointing toward tissue loss as mVF remains unaltered. In both cases, the GM VF changes are driven by local volume and not by net tissue changes. Together, these findings strongly point toward a morphological effect of the fluid redistribution on the GM, particularly at interfaces between tissue and CSF. These results additionally provide no sign of any GM or WM tissue loss in the temporal and frontal lobes or around the ventricles, which remained a possible explanation for previous results of VBM analyses. In addition, no net decrease in brain tissue after spaceflight was observed in any other region of the brain, with the exception of a small cluster located in the dura mater. However, this structure does not comprise brain tissue but has similar diffusional properties. This finding indicates a microstructural change in the dura mater, possibly related to the upward brain shift. Thus, our findings, based on the methodology of dMRI, show no evidence of neural tissue loss after spaceflight.

One remarkable observation is the GM mVF increase along a major part of the RTL at the border with the surrounding CSF. Considering the changes of different tissue types in the RTL, we found that the volume, the GM and CSF VFs, and mVFs all increased in this area. The CSF increases reflect the CSF space expansion in this area as noted earlier. Because the metric used to assess volume change is not specific to any of the tissue types in particular, the volume increase in these voxels can lead to the observed increase in GM mVF, while essentially, it may be more likely to correspond to the CSF expansion. However, in this case, we would have expected the GM VF to decrease in response to the CSF expansion, which we did not observe. This would have been more in line with the GM VF decreases observed along the expanded ventricles. One possible explanation is that the GM cortical layers of the RTL become more compact as a result of the expanded CSF space, leading to an increased GM fraction from a microscopic perspective. This might also explain previously observed GM volume decreases in the RTL through VBM analyses from a macroscopic perspective (*4*, *5*). Overall, morphological alterations seem more likely to explain the current and previous changes in the RTL. Supporting findings for this claim are that the effects are located at interfaces of tissue and CSF and that the significant voxels encompass a long-stretched contiguous area along multiple functional areas of the RTL. Future studies are required to investigate the exact modifications occurring within this area.

The changes between pre- and postflight described above are largely reversed 7 months after spaceflight. However, the recovery at the inferior part of the brain, including the ventricles, was overall less pronounced compared to the superior part of the brain, as some differences between preflight and follow-up remained significant. This is an expected finding, as our previously reported data at follow-up revealed a partly sustained ventricular expansion 7 months after return to Earth (*7*). Previous VBM analyses revealed a global CSF expansion in the whole subarachnoid space with concomitant GM volume decreases at follow-up (*4*), which suggests an incomplete recovery of the fluid shift–driven changes postflight. Our current results, however, do not point toward this global CSF expansion. Possibly, the higher resolution of the T1-weighted images used in the VBM analysis allows detecting more fine-grained changes compared to the dMRI modality. Hence, the global CSF expansion might occur rather in the "bulk" subarachnoid CSF space, which would be difficult to detect with our dMRI data, as most voxels in these regions also partly cover the adjacent GM.

Neuroplasticity of brain motor areas

Several of our results are indicative of neuroplasticity occurring as a result of spaceflight. Specifically, WM mVF increases of the cerebellum, parts of the corticospinal tract, and primary motor cortex, as well as GM mVF increases in the basal ganglia, provide evidence for motor system neuroplasticity. Supporting evidence includes the more focal localization of these changes, as opposed to the large-scale clusters showing significant GM VF and CSF changes. In addition, whereas these GM and CSF VF changes were found predominantly at the interface of GM and CSF, the WM and GM mVF increases in the motor structures are observed more deeply within the brain tissue. This is evident from the negligible CSF fractions in the ROIs where GM and WM mVF increased. Furthermore, an increase in tissue mVF reflects a net gain in the amount of the GM and WM tissue. Although the underlying cellular mechanisms to MRI-detectable findings are difficult to validate, these increases possibly point toward increased axonal packing, myelination, and/or astrocyte activation. These processes could contribute to MRI detectable signals as opposed to neuroplasticity processes at the synaptic level (*17*).

The cerebellum is involved in fine motor control, as well as in postural balance and oculomotor control, for which it receives vestibular and proprioceptive information (*18*). The cerebellum is even thought to play a role in gravity perception, as it provides a sense of verticality (*19*). The basal ganglia, on the other hand, play a role in

voluntary movement initiation (*20*), and the primary motor cortex serves as the main motor output center. These sensorimotor functions are seriously challenged in a microgravity environment, as impaired motor performance, postural control, and vestibular reflexes have been documented frequently after spaceflight (*21*–*23*). Moreover, both the cerebellum and basal ganglia are important substrates for learning behavior, which concerns error-driven adjustments in motor execution for the cerebellum (*24*) and implicit motor sequence learning for the basal ganglia (*25*). The structural changes in the cerebellum and basal ganglia might, therefore, reflect the required adjustments, suitable for sensorimotor processing in weightlessness. Even more, a recent review paper discusses the existence of direct anatomical connections between the cerebellum and basal ganglia, which might be important for sensorimotor adaptation (*26*).

Upon return to Earth, a readaptation is necessary for appropriate locomotion in Earth's 1G condition, which lasts several days to weeks as illustrated by several follow-up studies of sensorimotor control (*21*–*23*). Our whole-brain analyses suggest that a normalization to baseline levels has already taken place after 7 months back on Earth, while the analyses using ROIs show some remaining increases in tissue mVF in these sensorimotor areas, such as in the cerebellum. In this area, the WM mVF has partly normalized between postflight and follow-up but does not completely reach baseline levels. Assuming the tissue mVF increases are specific to motor adaptation processes in microgravity, it is possible that these partly reverse over time when returning to a 1G environment but also partly sustain as a reflection of long-term skill learning, which supports the observation that frequent flyers perform better at return than first-time flyers.

The few studies that previously have found signs of functional neuroplasticity after spaceflight have often observed changes in the activity of or connectivity with the cerebellum and primary motor cortex, although these changes have not yet been noted in the basal ganglia (*10*, *11*). In addition, one previous study has used dMRI to investigate changes in the brain as a result of long-duration spaceflight, and they found fractional anisotropy decreases in the cerebellum, which the authors ascribe to disrupted WM structural connectivity (*6*). However, fractional anisotropy is known to be misleading in regions containing crossing fibers (*27*). Our observations, on the other hand, more clearly demonstrate that a gain in WM tissue has occurred, pointing toward positive neuroplasticity rather than a disruption.

Clinical consequences

Regarding the clinical interpretation of the current and previous observations, recent hypotheses suggest that an upward brain shift might be a contributing factor for a hampered CSF resorption due to the compression of the major CSF absorption site in the superior sagittal sinus (*7*, *8*). The inability of CSF to reenter the vascular system would, therefore, cause an enlargement of the ventricles, acting as a buffer mechanism to store the accumulating CSF (*7*). Follow-up data show that this compression effect is relieved, as the net amount of CSF at the superior part of the brain appears to be restored. However, a remaining disturbance of CSF physiology is evident from the persistent enlargement of the ventricles and subarachnoid space (*4*, *7*), possibly pointing to a form of hysteresis. This raises questions on the exact timing of the relieved compression effect and the subsequent restoration of the affected CSF circulation.

Furthermore, the development of SANS is likely caused by alterations of the CSF circulation (*12*). Others have proposed a theoretical framework, which rather suggests that local mechanisms around the orbit are more likely to explain the occurrence of SANS (*28*). The intracranially accumulated CSF will reside in spaces that allow some extent of compliance, such as the ventricles. If these spaces are maximally expanded, CSF build-up in the retro-orbital space might take place, eventually leading to signs of SANS. Our data revealed that larger visual acuity decreases in cosmonauts postflight are associated with larger brain ventricular expansions. A possible explanation is that cosmonauts with smaller ventricular volume increases would have a remaining compliance capacity before CSF accumulation is able to cause effects associated with SANS. On the contrary, Roberts and colleagues (*16*) found that astronauts diagnosed with SANS showed smaller increases in ventricular volume compared to those who did not develop SANS. This would be attributable to an overall limited compliance capacity in astronauts with SANS (*29*, *30*). These seemingly contradicting findings highlight the need to prospectively address the link between SANS and changes in brain tissue and CSF compartments in a larger dataset, as these might be useful biomarkers to predict the occurrence of SANS. Moreover, note that all published literature on SANS concern NASA astronauts, while it has been claimed that SANS does not develop in Roscosmos cosmonauts (*31*). In this line, we hypothesize that different countermeasure schemes existing between the space crew populations could explain differences in ocular effects that eventually lead to SANS.

In previous work, the effects of spaceflight on the GM and WM tissue were reported (*4*, *5*), although without being able to provide clear information on what caused the observed changes. Understanding these effects on the GM and WM is essential, given the functional and behavioral implications that may arise from changes in the neural tissue. In this dMRI study, we found no net reductions in the amount of GM or WM, thus indicating that no neurodegeneration occurs as a result of long-duration spaceflight. In addition, the observed CSF VF increases occurred along the cortical folds or the ventricles, pertaining to the actual CSF compartments. The applied technique could have also detected free water changes localized within the neural tissue, which would pertain to the interstitial fluid and could reflect tissue damage. However, we did not observe these effects. The changes we observe in the GM and WM tissue either appear to result from morphological effects, which is unlikely to affect the actual brain function in the corresponding brain area, or to result from neuroplasticity, which serves as a natural adaptation process to a new environment.

The evidence of structural neuroplasticity provided in this work is likely to be considered as necessary changes in the brains of cosmonauts, as they adapt their motor strategies to the microgravity environment and readapt them to the conditions on Earth. Hence, we assume that the increases in tissue mVF observed in our study are not likely to have a negative clinical impact on the well-being of the cosmonauts but rather reflect positive adaptations. To confirm this assumption, the relation between these microstructural changes and functional performance, such as locomotion, should first be established. Furthermore, future work should also assess whether consecutive missions to space might determine the extent of net brain tissue increases, as experienced flyers are known to adapt better to microgravity and readapt faster when back on Earth than first-time flyers.

Limitations

Our study has several limitations, which are mostly inherent to the studied sample. First of all, we are studying a small sample size due to the low number of individuals engaging in long-duration space

missions lasting 6 months, as well as in the MRI experiment, with additional missing data at the follow-up time point. Nevertheless, to the best of our knowledge, this study includes the largest sample for studying brain structural changes after spaceflight in a prospective study design. Note that our findings are extremely consistent across cosmonauts and survive stringent multiple comparison corrections with a nonparametric statistical approach. Second, our sample contains a mix of first-time flyers and experienced flyers. Hence, the preflight data of experienced flyers might deviate from an actual baseline level, if effects from previous space missions persist. It is quite possible that spaceflight affects first-time flyers stronger than experienced flyers, a hypothesis that should be tested when sufficient data are acquired in both groups. Third, because of logistic reasons, we are only able to acquire postflight MRI data, on average, 9 days after the cosmonauts return. It is, therefore, likely that some or most effects measured are underestimations, suggesting that earlier scanning sessions could reveal more widespread and/or more pronounced effects of spaceflight on the brain. Last, one limitation beyond the studied population is the relatively low resolution of the dMRI images. While dMRI can provide more specific information on brain micro- and macrostructure compared to T1-weighted images, the voxel size of dMRI images is larger.

Conclusion

Our study reveals neural correlates of structural neuroplasticity of the sensorimotor system in cosmonauts after spaceflight, through the observation of net increases in GM tissue in the basal ganglia and in WM tissue in the cerebellum. We also confirmed previously observed fluid shift effects on the CSF and GM tissue but additionally provide evidence for the morphological nature of the GM tissue changes while, at the same time, showing no evidence of brain tissue loss. Seven months after the space mission, most early postflight changes recovered to preflight levels, although ventricular enlargement persisted and net GM or WM tissue remained increased to some degree in sensorimotor brain areas.

MATERIALS AND METHODS

Study design

Brain MRI data of 11 male Roscosmos cosmonauts who engaged in a long-duration space mission (average of 171 days) were acquired prospectively from February 2014 to March 2019 at the National Medical Research Treatment and Rehabilitation Centre of the Ministry of Health of Russia in Moscow, Russia. All cosmonauts were scanned before launch to the International Space Station (preflight) and after a mean of 9 days after return (postflight) to investigate the effect of spaceflight on the brain. Eight cosmonauts received an additional scan, on average, 239 days after return from spaceflight (follow-up) to assess whether the initial changes postflight returned to baseline. Pre- and postflight data of two subjects were acquired twice for two consecutive missions with a mean period of 1104 days (approximately 3 years) on Earth in between missions. Follow-up data were acquired for one of these two subjects, resulting in a total of 13 pre- and postflight measurements, as well as 9 follow-up measurements. Reasons for the missing data at the follow-up time points were the voluntary decision to discontinue the experiment for three cosmonauts and a pending follow-up measurement for one cosmonaut. In addition, 13 age-, gender- and education-matched control subjects were scanned twice with a similar time interval as that between the pre- and postflight scans to assess the effect of aging. All participants were right-handed, as assessed by the Edinburgh Handedness Inventory (*32*). An overview of the demographic information can be found in table S2.

The study was approved by the European Space Agency Medical Board, by the Committee of Biomedicine Ethics of the Institute of Biomedical Problems of the Russian Academy of Sciences and the Human Research Multilateral Review Board. All participants signed an informed consent form.

dMRI data acquisition

Data were acquired on a GE Discovery MR750 3T MRI system equipped with a 16-channel receiver head coil using a twice refocused pulsed gradient spin-echo echo-planar imaging sequence. An optimized multi-shell dMRI acquisition scheme was prescribed, containing diffusion weightings of $b = 0$, 700, 1200, and 2800 s/mm^2, applied in 8, 25, 45, and 75 directions, respectively (*15*). In addition, three $b = 0$ s/mm^2 images were acquired with reversed phase encoding, for the purpose of correcting susceptibility-induced distortions (*33*). Other imaging parameters were: repetition/echo time of 7800/100 ms, voxel size of 2.4 mm × 2.4 mm × 2.4 mm, matrix size of 100 × 100, 58 slices, and 1 excitation. Imaging was accelerated by a factor of 2 using the Array coil Spatial Sensitivity Encoding Technique. The total acquisition time was 21 min and 23 s.

In addition, T_1-weighted structural scans were acquired using a three-dimensional fast spoiled gradient-echo sequence to aid the identification of anatomical structures. Imaging parameters were repetition/echo time of 8/3 ms, flip angle of 12°, field of view of 240 mm, voxel size of 1 mm × 1 mm × 1 mm, matrix size of 240 × 240, 180 slices, and 1 excitation.

Data processing and analysis

dMRI data were processed and analyzed using a state-of-the-art pipeline (*34*) combining tools from MRtrix (www.mrtrix.org; version 0.3.RC2), FSL (http://fsl.fmrib.ox.ac.uk; version 6.0), and Advanced Normalization Tools (ANTs) (http://stnava.github.io/ANTs/; version 2.2.0).

Quality control

Consistency of imaging parameters throughout the entire study was ensured by automatically comparing the values of relevant Digital Imaging and Communications in Medicine (DICOM) attributes to their reference values. The correct interpretation of the gradient orientation information was ensured by adopting the approach of Jeurissen *et al.* (*35*). The quality of the dMRI images was assessed both automatically (*36*) and through visual inspection. No dMRI datasets were excluded from the study because of poor quality.

Preprocessing

To improve the quality of the raw dMRI images, they were corrected for several known artifacts. First, the images were denoised using random matrix theory to increase their signal-to-noise-ratio (*37*). Second, the Gibbs ringing artifact was suppressed on the basis of local subvoxel shifts to avoid spurious oscillations in the vicinity of sharp tissue boundaries (*38*). Next, susceptibility-induced distortions, as well as motion and Eddy current induced distortions, were corrected using an integrated approach (*39*). Then, the low-frequency intensity nonuniformity, also known as the bias field, was corrected (*40*). Last, dMRI images were upsampled spatially in

all three dimensions using cubic b-spline interpolation to a voxel size of 1.3 mm^3 to improve the accuracy of downstream spatial normalization.

Voxel-level modeling

From the preprocessed dMRI images, the full WM fiber orientation density function and the VF of GM- and CSF-like tissue were obtained using multi-tissue constrained spherical deconvolution with population-averaged tissue response functions (*15*). This technique operates on the idea that each tissue type in the brain has a distinct dMRI signal decay as a function of diffusion weighting strength. Hence, VFs, reflecting the relative contributions of WM-, GM-, and CSF-like tissue, can be teased apart within each voxel directly from the dMRI images without relying on spatial information or priors (fig. S7).

Spatial normalization

To achieve spatial correspondence between time points and participants, an unbiased study-specific group template was generated using a multilevel iterative nonlinear registration and averaging approach. At the first level, within-subject spatial correspondence was accomplished using iterative symmetric registration between the time points. At the second level, the time averages of all subjects underwent another iterative and symmetric registration procedure that ensures between-subject spatial correspondence (*41*, *42*). Last, tissue maps for CSF, GM, and WM VF were nonlinearly warped to the final population template in a single step to avoid the accumulation of interpolation errors. The complete normalization procedure is illustrated in fig. S7.

The resulting warped tissue VF are referred to as "unmodulated," as they do not take into account potential local volume differences between subjects or time points (*14*). However, as nonlinear warps used for spatial normalization are characterized by localized expansions and contractions of brain regions, it is important to also study and take into account these volumetric effects. To quantify local volumetric changes, we calculated the determinant of the Jacobian matrix (JDET), i.e., the warp's spatial derivative, at each voxel in the final nonlinear warp. In addition, the unmodulated VF maps were multiplied with JDET to obtain mVF maps.

Statistical analyses

We investigated changes in apparent tissue VF, tissue mVF, and volume at each voxel in the brain between preflight ($n = 13$), postflight ($n = 13$), and follow-up ($n = 9$). Statistical testing was performed using a general linear model (GLM) to compare time points in a paired design. Comparison of pre- and postflight data was performed on the full dataset ($n = 13$), while comparisons of the follow-up data with both pre- and postflight data were performed on the subset where data were available for all three time points ($n = 9$). The time delays between the return to Earth and both the postflight and follow-up scan sessions were treated as nuisance variables. In addition, pre- to postflight differences in cosmonauts were compared to the differences of two time points with a similar time interval in a matched control group. Similarly, a GLM was used to compare cosmonauts and controls using a two-sample unpaired *t* test of the differences in time. For both paired and unpaired *t* tests, threshold-free cluster enhancement (TFCE) was applied to the resulting *t* statistic maps (*43*). Final *P* values were obtained through nonparametric permutation testing (8192 permutations) with FWE correction and a significance threshold of $P < 0.05$. Before voxel-based statistical analysis, a Gaussian smoothing kernel with a full width at half maximum of only 2.4 mm was applied to increase the signal-to-noise ratio while preserving the specificity of the anatomical localization. The same smoothing kernel was used to perform variance smoothing during nonparametric statistical analysis to increase the statistical power at low sample sizes (*44*).

Potential differences between cosmonauts and controls regarding age and the time interval between scans (between pre- and postflight for cosmonauts) were statistically tested using a nonparametric two-tailed Mann-Whitney *U* test. Results were considered statistically significant if $P < 0.05$.

ROI analysis

Several ROIs were defined to summarize tissue changes across time. First, the mean GM, WM, and CSF mVF across the whole brain was obtained, using a brain mask of all voxels present in all subjects. Next, we used the Neuromorphometrics atlas (https://masi.vuse.vanderbilt.edu/workshop2012/index.php/Challenge_Details; www.oasis-brains.org/; and http://Neuromorphometrics.com/) to obtain parcels of the third, fourth, and lateral ventricles, in which the mean CSF mVF was calculated and evaluated across time. Since we summarized tissue values in independent ROIs, we performed additional statistical tests to investigate significant effects within these regions. Linear mixed models were used to test for an effect of time on the tissue parameters in the whole brain and the ventricles of cosmonauts. Time was considered a fixed effect, while subject was a random effect, using a random intercept model. Results were significant if $P < 0.05$, and if so, Tukey's post hoc test was used to investigate between which pair of time points there was a significant difference. The significance threshold was set at $P < 0.05$. In addition, the difference between pre- and postflight in cosmonauts and between the two time point measurements in the control group were calculated to test for differences between groups using a Mann-Whitney *U* test. The significance threshold was set at $P < 0.05$.

Six ROIs were created on the basis of the voxel-based results between pre- and postflight in cosmonauts to quantify the changes in VF and mVF of different tissue types within the same area. The median across voxels was calculated in each ROI, and for each subject and time point, which was performed for the apparent GM, WM, and CSF VF and mVF. Subsequently, the median of all within-subject differences between time points was calculated. For volume, the median JDET ratio of the two time points was calculated, which renders the multiplication factor by which the volume changed across time points.

Visual acuity data

We retrospectively included visual acuity scores of all cosmonauts before and 3 days after spaceflight of both left and right eyes. All tests were conducted in the morning. Subjects were presented with Sivtsev's tables using the Rotta apparatus at a distance of 5 m. A score of 1 represents the healthy population norm, with higher scores corresponding to better visual acuity. The difference in visual acuity score between pre- and postflight was calculated, rendering negative values for visual acuity decreases at postflight compared to preflight. Statistical analysis was performed for the visual acuity score of the right and left eyes separately by means of a two-tailed exact Wilcoxon signed-rank test. The significance threshold was set at $P < 0.05$.

A voxel-based correlation analysis was performed between the relative pre- and postflight differences in mVF of CSF and the pre- to postflight difference in visual acuity for both eyes separately.

TFCE was applied to the resulting statistical maps using nonparametric permutation testing with 8192 permutations. The significance threshold was set at $P < 0.05$ after cluster-level FWE correction.

Kendall's tau nonparametric correlation test was performed between the pre- to postflight difference in visual acuity for both eyes separately and the pre- to postflight difference in CSF mVF of lateral ventricles, third ventricle, the superior, and inferior CSF interface ROIs. The significance threshold was set at $P < 0.05$.

SUPPLEMENTARY MATERIALS

Supplementary material for this article is available at http://advances.sciencemag.org/cgi/content/full/6/36/eaaz9488/DC1

View/request a protocol for this paper from *Bio-protocol*.

REFERENCES AND NOTES

1. G. Clément, *Fundamentals of Space Medicine* (Springer, ed. 2, 2011).
2. P.-M. Lledo, M. Alonso, M. S. Grubb, Adult neurogenesis and functional plasticity in neuronal circuits. *Nat. Rev. Neurosci.* **7**, 179–193 (2006).
3. A. Van Ombergen, S. Laureys, S. Sunaert, E. Tomilovskaya, P. M. Parizel, F. L. Wuyts, Spaceflight-induced neuroplasticity in humans as measured by MRI: What do we know so far? *NPJ Microgravity* **3**, 2 (2017).
4. A. Van Ombergen, S. Jillings, B. Jeurissen, E. Tomilovskaya, R. M. Rühl, A. Rumshiskaya, I. Nosikova, L. Litvinova, J. Annen, E. V. Pechenkova, I. B. Kozlovskaya, S. Sunaert, P. M. Parizel, V. Sinitsyn, S. Laureys, J. Sijbers, P. Zu Eulenburg, F. L. Wuyts, Brain tissue–volume changes in cosmonauts. *N. Engl. J. Med.* **379**, 1678–1680 (2018).
5. V. Koppelmans, J. J. Bloomberg, A. P. Mulavara, R. D. Seidler, Brain structural plasticity with spaceflight. *NPJ Microgravity* **2**, 2 (2016).
6. J. K. Lee, V. Koppelmans, R. F. Riascos, K. M. Hasan, O. Pasternak, A. P. Mulavara, J. J. Bloomberg, R. D. Seidler, Spaceflight-associated brain white matter microstructural changes and intracranial fluid redistribution. *JAMA Neurol.* **76**, 412–419 (2019).
7. A. Van Ombergen, S. Jillings, B. Jeurissen, E. Tomilovskaya, A. Rumshiskaya, L. Litvinova, I. Nosikova, E. Pechenkova, I. Rukavishnikov, O. Manko, S. Danylichev, R. M. Rühl, I. B. Kozlovskaya, S. Sunaert, P. M. Parizel, V. Sinitsyn, S. Laureys, J. Sijbers, P. Z. Eulenburg, F. L. Wuyts, Brain ventricular volume changes induced by long-duration spaceflight. *Proc. Natl. Acad. Sci. U.S.A.* **116**, 10531–10536 (2019).
8. D. R. Roberts, M. H. Albrecht, H. R. Collins, D. Asemani, A. R. Chatterjee, M. V. Spampinato, X. Zhu, M. I. Chimowitz, M. U. Antonucci, Effects of spaceflight on astronaut brain structure as indicated on MRI. *N. Engl. J. Med.* **377**, 1746–1753 (2017).
9. N. Alperin, A. M. Bagci, S. H. Lee, Spaceflight-induced changes in white matter hyperintensity burden in astronauts. *Neurology* **89**, 2187–2191 (2017).
10. A. Demertzi, A. Van Ombergen, E. Tomilovskaya, B. Jeurissen, E. Pechenkova, C. Di Perri, L. Litvinova, E. Amico, A. Rumshiskaya, I. Rukavishnikov, J. Sijbers, V. Sinitsyn, I. B. Kozlovskaya, S. Sunaert, P. M. Parizel, P. H. Van de Heyning, S. Laureys, F. L. Wuyts, Cortical reorganization in an astronaut's brain after long-duration spaceflight. *Brain Struct. Funct.* **221**, 2873–2876 (2016).
11. E. Pechenkova, I. Nosikova, A. Rumshiskaya, L. Litvinova, I. Rukavishnikov, E. Mershina, V. Sinitsyn, A. Van Ombergen, B. Jeurissen, S. Jillings, S. Laureys, J. Sijbers, A. Grishin, L. Chernikova, I. Naumov, L. Kornilova, F. L. Wuyts, E. Tomilovskaya, I. Kozlovskaya, Alterations of functional brain connectivity after long-duration spaceflight as revealed by fMRI. *Front. Physiol.* **10**, 761 (2019).
12. T. H. Mader, C. R. Gibson, N. R. Miller, P. S. Subramanian, N. B. Patel, A. G. Lee, An overview of spaceflight-associated neuro-ocular syndrome (SANS). *Neurol. India* **67**, S206–S211 (2019).
13. J. Ashburner, K. J. Friston, Voxel-Based Morphometry—The Methods. *Neuroimage* **11**, 805–821 (2000).
14. D. A. Raffelt, J.-D. Tournier, R. E. Smith, D. N. Vaughan, G. Jackson, G. R. Ridgway, A. Connelly, Investigating white matter fibre density and morphology using fixel-based analysis. *Neuroimage* **144**, 58–73 (2017).
15. B. Jeurissen, J.-D. Tournier, T. Dhollander, A. Connelly, J. Sijbers, Multi-tissue constrained spherical deconvolution for improved analysis of multi-shell diffusion MRI data. *Neuroimage* **103**, 411–426 (2014).
16. D. R. Roberts, D. Asemani, P. J. Nietert, M. A. Eckert, D. C. Inglesby, J. J. Bloomberg, M. S. George, T. R. Brown, Prolonged microgravity affects human brain structure and function. *AJNR Am. J. Neuroradiol.* **40**, 1878–1885 (2019).
17. Y. Sagi, I. Tavor, S. Hofstetter, S. Tzur-Moryosef, T. Blumenfeld-Katzir, Y. Assaf, Learning in the fast lane: New insights into neuroplasticity. *Neuron* **73**, 1195–1203 (2012).
18. D. Manzoni, The cerebellum may implement the appropriate coupling of sensory inputs and motor responses: Evidence from vestibular physiology. *Cerebellum* **4**, 178–188 (2005).
19. P. R. MacNeilage, S. Glasauer, Gravity perception: The role of the cerebellum. *Curr. Biol.* **28**, R1296–R1298 (2018).
20. K. R. Bailey, R. G. Mair, The role of striatum in initiation and execution of learned action sequences in rats. *J. Neurosci.* **26**, 1016–1025 (2006).
21. G. Courtine, T. Pozzo, Recovery of the locomotor function after prolonged microgravity exposure. I. Head-trunk movement and locomotor equilibrium during various tasks. *Exp. Brain Res.* **158**, 86–99 (2004).
22. A. P. Mulavara, A. H. Feiveson, J. Fiedler, H. Cohen, B. T. Peters, C. Miller, R. Brady, J. J. Bloomberg, Locomotor function after long-duration space flight: Effects and motor learning during recovery. *Exp. Brain Res.* **202**, 649–659 (2010).
23. E. Hallgren, L. Kornilova, E. Fransen, D. Glukhikh, S. T. Moore, G. Clément, A. Van Ombergen, H. MacDougall, I. Naumov, F. L. Wuyts, Decreased otolith-mediated vestibular response in 25 astronauts induced by long-duration spaceflight. *J. Neurophysiol.* **115**, 3045–3051 (2016).
24. L. S. Popa, T. J. Ebner, Cerebellum, predictions and errors. *Front. Cell. Neurosci.* **12**, 524 (2019).
25. A. Karabanov, S. Cervenka, O. de Manzano, H. Forssberg, L. Farde, F. Ullen, Dopamine D2 receptor density in the limbic striatum is related to implicit but not explicit movement sequence learning. *Proc. Natl. Acad. Sci. U.S.A.* **107**, 7574–7579 (2010).
26. A. C. Bostan, P. L. Strick, The basal ganglia and the cerebellum: Nodes in an integrated network. *Nat. Rev. Neurosci.* **19**, 338–350 (2018).
27. B. Jeurissen, A. Leemans, J.-D. Tournier, D. K. Jones, J. Sijbers, Investigating the prevalence of complex fiber configurations in white matter tissue with diffusion magnetic resonance imaging. *Hum. Brain Mapp.* **34**, 2747–2766 (2013).
28. P. Wostyn, T. H. Mader, C. R. Gibson, H. E. Killer, The escape of retrobulbar cerebrospinal fluid in the astronaut's eye: Mission impossible? *Eye* **33**, 1519–1524 (2019).
29. A. Van Ombergen, S. Jillings, E. Tomilovskaya, F. L. Wuyts, P. Z. Eulenburg, Reply to Wostyn et al.: Investigating the spaceflight-associated neuro-ocular syndrome and the human brain in lockstep. *Proc. Natl. Acad. Sci. U.S.A.* **116**, 15772–15773 (2019).
30. L. A. Kramer, K. M. Hasan, A. E. Sargsyan, J. S. Wolinsky, D. R. Hamilton, R. F. Riascos, W. K. Carson, J. Heimbigner, V. S. Patel, S. Romo, C. Otto, MR-derived cerebral spinal fluid hydrodynamics as a marker and a risk factor for intracranial hypertension in astronauts exposed to microgravity. *J. Magn. Reson. Imaging* **42**, 1560–1571 (2015).
31. V. V. Bogomolov, M. P. Kuzmin, S. N. Danilichev, On the intracranial hypertension in astronauts during long-term microgravity. *Aviakosm. Ekolog. Med.* **49**, 54–58 (2015).
32. R. C. Oldfield, The assessment and analysis of handedness: The Edinburgh inventory. *Neuropsychologia* **9**, 97–113 (1971).
33. J. L. R. Andersson, S. Skare, J. Ashburner, How to correct susceptibility distortions in spin-echo echo-planar images: Application to diffusion tensor imaging. *Neuroimage* **20**, 870–888 (2003).
34. J.-D. Tournier, R. Smith, D. Raffelt, R. Tabbara, T. Dhollander, M. Pietsch, D. Christiaens, B. Jeurissen, C.-H. Yeh, A. Connelly, *MRtrix3*: A fast, flexible and open software framework for medical image processing and visualisation. *Neuroimage* **202**, 116137 (2019).
35. B. Jeurissen, A. Leemans, J. Sijbers, Automated correction of improperly rotated diffusion gradient orientations in diffusion weighted MRI. *Med. Image Anal.* **18**, 953–962 (2014).
36. M. Bastiani, M. Cottaar, S. P. Fitzgibbon, S. Suri, F. Alfaro-Almagro, S. N. Sotiropoulos, S. Jbabdi, J. L. R. Andersson, Automated quality control for within and between studies diffusion MRI data using a non-parametric framework for movement and distortion correction. *Neuroimage* **184**, 801–812 (2019).
37. J. Veraart, D. S. Novikov, D. Christiaens, B. Ades-Aron, J. Sijbers, E. Fieremans, Denoising of diffusion MRI using random matrix theory. *Neuroimage* **142**, 394–406 (2016).
38. E. Kellner, B. Dhital, V. G. Kiselev, M. Reisert, Gibbs-ringing artifact removal based on local subvoxel-shifts. *Magn. Reson. Med.* **76**, 1574–1581 (2016).
39. J. L. R. Andersson, S. N. Sotiropoulos, An integrated approach to correction for off-resonance effects and subject movement in diffusion MR imaging. *Neuroimage* **125**, 1063–1078 (2016).
40. N. J. Tustison, B. B. Avants, P. A. Cook, Y. Zheng, A. Egan, P. A. Yushkevich, J. C. Gee, N4ITK: Improved N3 bias correction. *IEEE Trans. Med. Imaging* **29**, 1310–1320 (2010).
41. D. Raffelt, J.-D. Tournier, J. Fripp, S. Crozier, A. Connelly, O. Salvado, Symmetric diffeomorphic registration of fibre orientation distributions. *Neuroimage* **56**, 1171–1180 (2011).
42. M. Pietsch, D. Christiaens, J. Hutter, L. Cordero-Grande, A. N. Price, E. Hughes, A. D. Edwards, J. V. Hajnal, S. J. Counsell, J.-D. Tournier, A framework for multi-component analysis of diffusion MRI data over the neonatal period. *Neuroimage* **186**, 321–337 (2019).
43. S. M. Smith, T. E. Nichols, Threshold-free cluster enhancement: Addressing problems of smoothing, threshold dependence and localisation in cluster inference. *Neuroimage* **44**, 83–98 (2009).
44. T. E. Nichols, A. P. Holmes, Nonparametric permutation tests for functional neuroimaging: A primer with examples. *Hum. Brain Mapp.* **15**, 1–25 (2002).

Acknowledgments: This paper is dedicated to I. B. Kozlovskaya (1927–2020) who supported vigorously the concept of neuroplasticity in cosmonauts and devoted her life to space physiology and adaptation to weightlessness. **Funding:** This work was supported by

ESA Grant ISLRA 2009-1062, Russian Academy of Sciences (grant number 63.1), Belgian Science Policy Prodex, the Research Foundation Flanders (FWO Vlaanderen) (to A.V.O. and B.J.), French Speaking Community Concerted Research Action Grant ARC06/11-340, German Federal Ministry of Education and Research Grant 01 EO 0901 (to P.z.E.), and Zonta International Amelia Earhart Fellowship 2016–2017 (to A.V.O.). B.J. is a postdoctoral fellow for FWO Vlaanderen; S.L. is a research director at the Fonds de la Recherche Scientifique.
Author contributions: E.T., I.B.K, S.S., P.M.P., S.L., J.S., F.L.W., and B.J. contributed to the conception of the work. A.V.O., E.T., A.R., E.P., I.R., I.B.K., S.S., P.M.P., V.S., S.L., J.S., F.L.W., and B.J. contributed to the design of the work. A.V.O., A.R., L.L., I.N., E.P., I.R., I.B.K., O.M., S.D., V.S., V.P., F.L.W., and B.J. contributed to the data acquisition. S.J. and B.J. contributed to data analysis. S.J., A.V.O., E.P., P.z.E., F.L.W., and B.J. contributed to data interpretation. B.J. contributed to software creation. S.J. and B.J. contributed to drafting the manuscript. A.V.O., E.P., P.z.E., and F.L.W. contributed to substantial revision of the manuscript. **Competing interests:** The authors declare they have no competing interests. **Data and materials availability:** All data needed to evaluate the conclusions in the paper are present in the paper and/or the Supplementary Materials. Additional data related to this paper may be requested from the authors.

Submitted 29 October 2019
Accepted 15 July 2020
Published 4 September 2020
10.1126/sciadv.aaz9488

Citation: S. Jillings, A. Van Ombergen, E. Tomilovskaya, A. Rumshiskaya, L. Litvinova, I. Nosikova, E. Pechenkova, I. Rukavishnikov, I. B. Kozlovskaya, O. Manko, S. Danilichev, S. Sunaert, P. M. Parizel, V. Sinitsyn, V. Petrovichev, S. Laureys, P. zu Eulenburg, J. Sijbers, F. L. Wuyts, B. Jeurissen, Macro- and microstructural changes in cosmonauts' brains after long-duration spaceflight. *Sci. Adv.* **6**, eaaz9488 (2020).

Science Advances

Macro- and microstructural changes in cosmonauts' brains after long-duration spaceflight

Steven Jillings, Angelique Van Ombergen, Elena Tomilovskaya, Alena Rumshiskaya, Liudmila Litvinova, Inna Nosikova, Ekaterina Pechenkova, Ilya Rukavishnikov, Inessa B. Kozlovskaya, Olga Manko, Sergey Danilichev, Stefan Sunaert, Paul M. Parizel, Valentin Sinitsyn, Victor Petrovichev, Steven Laureys, Peter zu Eulenburg, Jan Sijbers, Floris L. Wuyts and Ben Jeurissen

Sci Adv **6** (36), eaaz9488.
DOI: 10.1126/sciadv.aaz9488

Science Advances (ISSN 2375-2548) is published by the American Association for the Advancement of Science, 1200 New York Avenue NW, Washington, DC 20005. The title *Science Advances* is a registered trademark of AAAS.